AJNR

Frequencies Contributing to Functional Connectivity in the Cerebral Cortex in "Resting-state" Data

Dietmar Cordes, Victor M. Haughton, Konstantinos Arfanakis, John D. Carew, Patrick A. Turski, Chad H. Moritz, Michelle A. Quigley and M. Elizabeth Meyerand

Frequencies Contributing to Functional Connectivity in the Cerebral Cortex in "Resting-state" Data

Dietmar Cordes, Victor M. Haughton, Konstantinos Arfanakis, John D. Carew, Patrick A. Turski, Chad H. Moritz, Michelle A. Quigley, and and M. Elizabeth Meyerand

BACKGROUND AND PURPOSE: In subjects performing no specific cognitive task ("resting state"), time courses of voxels within functionally connected regions of the brain have high cross-correlation coefficients ("functional connectivity"). The purpose of this study was to measure the contributions of low frequencies and physiological noise to cross-correlation maps.

METHODS: In four healthy volunteers, task-activation functional MR imaging and resting-state data were acquired. We obtained four contiguous slice locations in the "resting state" with a high sampling rate. Regions of interest consisting of four contiguous voxels were selected. The correlation coefficient for the averaged time course and every other voxel in the four slices was calculated and separated into its component frequency contributions. We calculated the relative amounts of the spectrum that were in the low-frequency (0 to 0.1 Hz), the respiratory-frequency (0.1 to 0.5 Hz), and cardiac-frequency range (0.6 to 1.2 Hz).

RESULTS: For each volunteer, resting-state maps that resembled task-activation maps were obtained. For the auditory and visual cortices, the correlation coefficient depended almost exclusively on low frequencies (<0.1 Hz). For all cortical regions studied, low-frequency fluctuations contributed more than 90% of the correlation coefficient. Physiological (respiratory and cardiac) noise sources contributed less than 10% to any functional connectivity MR imaging map. In blood vessels and cerebrospinal fluid, physiological noise contributed more to the correlation coefficient.

CONCLUSION: Functional connectivity in the auditory, visual, and sensorimotor cortices is characterized predominantly by frequencies slower than those in the cardiac and respiratory cycles. In functionally connected regions, these low frequencies are characterized by a high degree of temporal coherence.

Time-series data from MR imaging of functionally related regions of the brain show a high degree of temporal coherence of low-frequency fluctuations (1–6). Phase coherence of blood flow fluctuations between anatomically different but functionally related regions implies neuronal connections or functional connectivity between these regions. Functional connectivity has been reported in portions of the sensorimotor, auditory, and visual systems. These synchronous fluctuations may represent changes in local blood flow secondary to fluctuations in firing rates within large distributed neural networks (1). Functional connectivity has been shown in subjects performing no specific cognitive task ("resting state") and in subjects performing tasks that did not activate regions in which functional connectivity was measured (7).

In the resting state, functional connectivity MR (fcMR) imaging, a map of the temporal correlations of MR signal time courses, is computed by specifying a region of interest (ROI) in a functional area and cross-correlating it with all other voxel time courses in the brain. Unlike conventional functional MR (fMR) imaging, no specific task is prescribed for the subject. The fcMR study provides a new way to measure the interdependency of brain regions and assess the strength of neuronal connections.

Although the feasibility of fcMR has been shown, functional connectivity is incompletely characterized, and fcMR methods are not yet optimized. The frequencies at which physiological fluctuations can be detected have not been thoroughly investigated. In many studies, low sampling rates were employed in acquisition of echo-planar images, which might fail to characterize respiratory

and cardiac frequencies. For example, at a sampling interval of TR = 2 s, the frequency bands 0.4–0.6 Hz and 0.9–1.1 Hz will appear artifactually (because of bulk motion and fluctuations in signal intensity reflecting cardiac or respiratory cycles) in the low-frequency range (<0.1 Hz). Simulation of low-frequency fluctuations by such ''aliasing'' of cyclic changes at the respiratory or cardiac rate has not been excluded. Therefore, the specificity of the functional connectivity map has been questioned. The use of low-pass filters in some studies has reduced physiological noise sources but also has obscured any frequency-specific information in those noise sources (3). The power spectrum of voxel time courses has been analyzed (8), but, because the power spectrum contains no phase information, this analysis cannot measure the contribution of each frequency in a voxel time course to the overall fcMR map. For example, two voxel time courses with identical power spectra can be uncorrelated. Also, the frequency content in a voxel time course defines the degrees of freedom. Choosing an ROI that contains voxel time courses with drastically different degrees of freedom can lead to less specific fcMR maps.

The purpose of this study was to calculate the contribution of each frequency to resting-state cross-correlation maps. Multislice acquisitions with a rapid sampling rate (TR, 400 ms) were used to eliminate or reduce aliasing. To measure the contribution of the frequency to the cross-correlation coefficient, we use an established expression for the spectral distribution of the cross-correlation coefficient (6). The spectral analysis of the correlation coefficient shows which frequencies contribute to interregional functional connectivity. We hypothesized that, on average, only frequencies less than 0.1 Hz contribute significantly to interregional functional connectivity, and respiratory and cardiac noise contribute minimally to fcMR maps. We calculated the spectral compositions for auditory, visual, and sensorimotor tasks in a series of volunteers. To our knowledge, functional connectivity has not been analyzed in this way.

Methods

Four volunteers, aged 20 to 25 years and claiming to be in good health with no history of neurologic illness, were recruited as participants for the fMR experiment. Consent was obtained according to institutional guidelines.

Each subject underwent the same series of scans performed with a 1.5-T commercial MR scanner equipped with high-speed gradients and a standard birdcage head coil. Head stabilization and motion control were achieved by using foam pads. First, high-resolution, whole-brain anatomic images were obtained with 2D multislice, spin-echo sequences (coronal plane, 20 slices, 256 × 128 matrix, TR/TE of 500/8, field of view of 24 cm, slice thickness of 7 mm, and interslice gap of 2 mm). In addition, a 3D spoiled gradient-recalled whole-brain–volume scan was acquired (axial plane, 124 slices, 256 × 128 matrix, TR/TE of 21/7, flip angle of 40°, field of view of 24 cm, slice thickness of 1.1 mm, and no gap). For conventional task-activation fMR imaging, a series of 148 time

frames was acquired with single-shot gradient-recalled echo-planar imaging in the coronal plane (20 slices, 64 × 64 matrix, flip angle of 82°, TR/TE of 2000/50, field of view of 24 cm, receiver bandwidth of 125 kHz, slice thickness of 7 mm, and interslice gap of 2 mm). For the resting-state fcMR imaging studies, the technical acquisition parameters were the same, except the TR was reduced to 400 ms with a 50° flip angle, allowing four slices to be scanned, and the number of time frames was increased to 1300 to achieve a reliable statistic. In each echo-planar imaging series, the images belonging to the first four (for fMR) or 20 (for fcMR) time frames were discarded because the MR signal was not stationary. Voxel dimensions were 3.75 × 3.75 × 7 mm³ (x, y, z). The cardiac and respiratory rates were recorded using a pulse oximeter and a flexible respiratory belt.

For fMR (''task-acquisition''), the subject performed a specific task for four 32-second periods, each separated by 32-second periods of rest. Each volunteer performed each of three tasks: listening to narrated text, viewing of a strobe light, and finger tapping. For the auditory task, the subject listened to a recorded text by air-driven headphones. For visual cortex activation, the subject viewed a strobe light with flashing frequency of 8 Hz. The finger-tapping task was self-paced, bilateral apposition of the thumb and other fingers in a sequential pattern.

For the fcMR (''resting acquisition''), the subject was instructed to rest, be as motionless as possible, keep eyes closed, and perform no specific cognitive exercise during the entire scan. fcMR imaging was performed after the fMR imaging.

The echo-planar raw data were filtered in the spatial frequency domain with a low-pass Hamming filter to increase the signal-to-noise ratio (9). Images were checked for motion by using a 3D registration program included in AFNI (Robert Cox, Medical College of Wisconsin). All subjects had less than 0.4-mm maximum displacement in x, y, or z. Motion correction of echo-planar data was not performed because all motion-correction algorithms tend to increase spatial correlations to an unknown degree.

For fMR, the time course was analyzed with a locally developed program (10, 11). A least-squares fitting algorithm was used to compare the observed data on a voxel-by-voxel basis against a constant (baseline signal intensity), a ramp (signal drift), and a boxcar function (idealized expected response to the task or stimulus). The boxcar function had a unit amplitude and a period that matched the on/off cycles of the task or stimulus, smoothed by convolution with a Poisson function (with a 6-second mean) to account for hemodynamic delay. The amplitude and the uncertainty of the fit to the boxcar reference function were calculated by least-squares minimization. A t score was calculated and converted to a z score. An overall adjusted P value was determined to address levels of significance. All voxels with $P < .001$ were merged with coregistered anatomic images.

For fcMR imaging, ROIs consisting of 2 × 2 ''seed'' voxels were selected in the primary auditory cortex, striate cortex, or in the Rolandic cortex by referring to the maximum task activation seen in the fMR for each of the tasks. For comparison, several other seed voxels were selected in other regions where functional connectivity was not anticipated and where the cardiac and respiratory effects were expected. These regions were in the right internal carotid artery, the left internal jugular vein, and in the cerebrospinal fluid (left lateral ventricle). The correlation coefficients of the seed voxels and every other voxel within the four slices of the brain were calculated.

A nonparametric, multiple-comparisons procedure was used to compute the statistical significance of fcMR maps (12, 13). To arrive at a null statistic for resting-state data, the time course of the seed voxel or cluster was altered by randomization of the phase of its complex Fourier components, an approach that does not change the power spectrum. The null distribution of correlation coefficients for a particular seed vox-
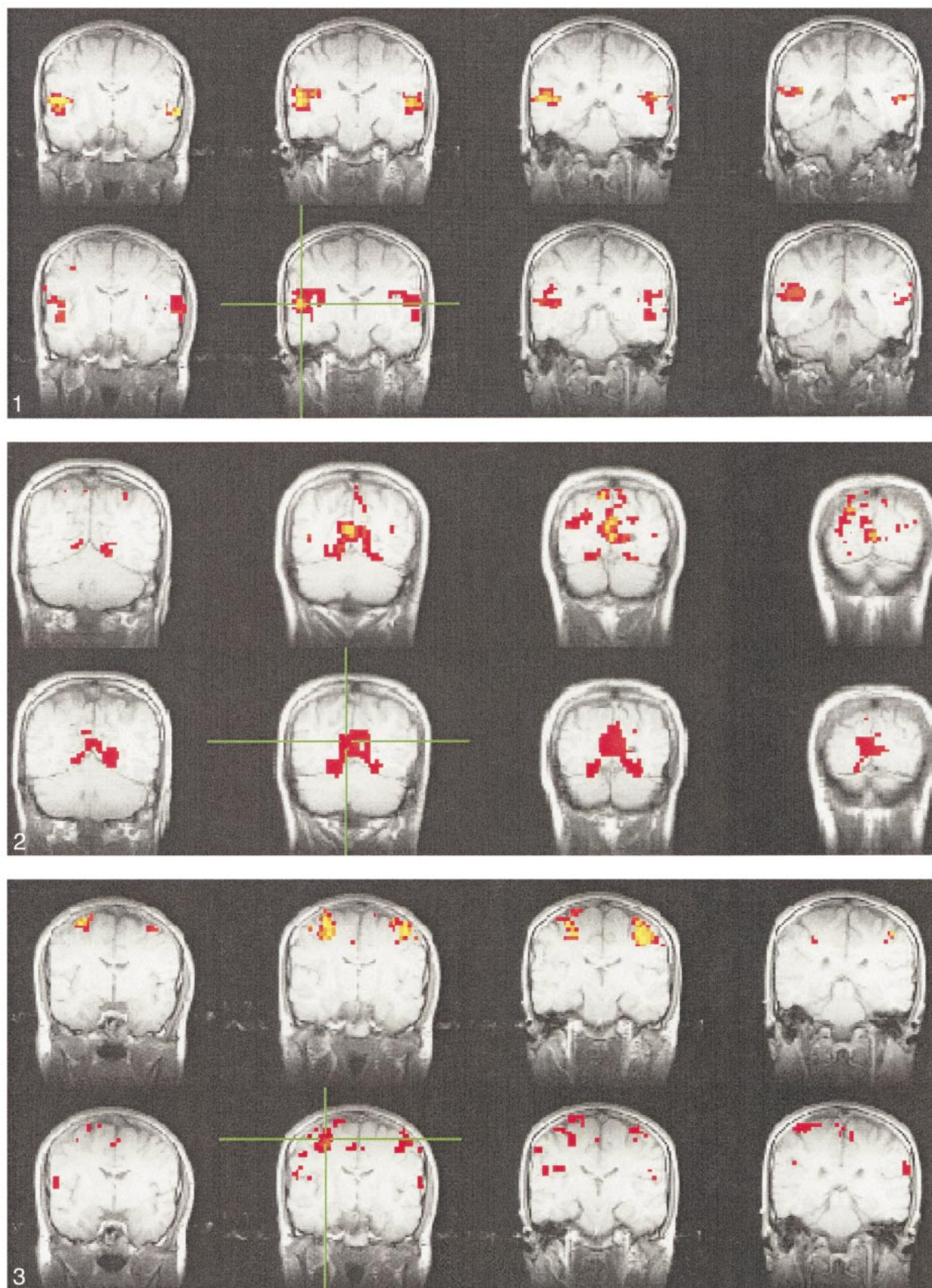
FIG 1.   Consecutive coronal fMR maps of voxels activated by a text-listening task (top) and of the voxels functionally connected with a 2 × 2-seed voxel ROI (*crosshairs*) within the auditory cortex during resting-state (bottom). Task activation is evident in the region of the primary and association auditory cortices in the superior temporal lobe. Many of the voxels functionally connected with the seed voxels in the left auditory cortex (*crosshairs*) have a similar distribution. All maps are representative and are from a single subject.

el or cluster then was obtained by calculating all possible cross-correlation coefficients between the seed voxel after phase randomization and all other voxels in the brain. This approach assigned an overall adjusted P value to each cross-correlation value, when carried out for each seed voxel or cluster. All fcMR maps then were subjected to a $P = .005$ threshold. The corresponding cross-correlation coefficients (using 1300 time frames) were in the range of 0.5–0.8, depending on the seed voxel or cluster. The degrees of freedom of the seed voxel or cluster were computed by Friston's method (14). Voxels correlating significantly were merged with anatomic images. The locations of the voxels in the fcMR were compared with the location of task activation in the fMR.

The average frequency spectrum of the correlation coefficients was computed for each fcMR map by expressing the voxel time courses in terms of their inverse Fourier transforms and calculating the cross-correlation coefficient in frequency (ie, Fourier) space. The expression for the contribution of the nth frequency to the total correlation coefficient (cc) is:

$$cc_n = \frac{N(\mathrm{Re}(\omega_n)\mathrm{Re}(\lambda_n) + \mathrm{Im}(\omega_n)\mathrm{Im}(\lambda_n))}{D}$$

such that

$$cc = \sum_{n=1}^{N-1} cc_n,$$

where ω_n and λ_n are the complex frequencies of the voxel-time courses of the seed voxel $f(t)$ and voxel $g(t)$, $n \in [0,N-1]$, and N is the number of discrete time points. The term $n = 0$ does not contribute to cc because the mean has been removed from $f(t)$ and $g(t)$. The denominator D represents a normalization factor (for details see [6]). To address the spectral distribution of the cross-correlation coefficient in a fcMR map, the average value $<cc_n>$ is computed by using all voxel time courses that give significant correlations with a P value of $\geq.005$.

Results

In the fMR experiments, significant activations at the $P = .001$ level were found bilaterally in the superior temporal lobe and insular region (passive text-listening task), in the striate cortex (visual task), the somatosensory cortex, and the supplementary motor area (SMA) and dentate nuclei of the cerebellum (motor task). These regions of activations were very consistent in all subjects.

For the fcMR resting-state maps, all subjects showed fairly symmetrical functional connectivity across hemispheres at a P value of .005 for the motor, auditory, and visual regions. The fcMR maps resembled closely the fMR task-activation pattern. However, some voxels of the fcMR maps did not match those of the task-activation maps, even after adjusting the threshold. For example, no functional connectivity between the somatosensory cortex and the dentate nuclei in the cerebellum was found, although both areas were activated in the motor task. In general, fcMR maps appeared to be noisier than fMR maps, indicating non-stationary fluctuations in the data. However, the appearance of the maps was similar between individuals. Increasing the threshold of the fcMR maps to equalize the P values between task-activation and resting-state maps reduced the noise in the images but also reduced the extent of the spatial maps.

Figures 1–4 show typical examples of task-activation maps and resting-state fcMR maps for four contiguous slices. Auditory cortex activation and functional connectivity showed very similar spatial distributions across different slices (Fig 1). The fcMR maps did not vary markedly as the ROI was moved within the region of activation in the superior temporal gyrus. Activation in the striate cortex also showed close resemblance to the resting-state fcMR map (Fig 2). The fcMR map proved also to be fairly robust when the seed voxels were moved within the primary visual cortex. Similarly, somatosensory activation and the corresponding resting-state fcMR map showed close resemblance between left and right hemispheric symmetry (Figs 3 and 4). However, more of the SMA was identified in the fcMR than in the task activation from finger tapping. In general, voxels selected randomly outside regions that were activated by a task showed no significant correlation with voxels in the sensorimotor, auditory, and visual regions.

In Figures 5–7, the spectral distribution of the cross-correlation coefficient is shown for auditory, visual, and motor resting-state fcMR maps. For functional connectivity of the auditory cortex (Fig 5) or visual cortex (Fig 6), only low frequencies (<0.1 Hz) contributed to the correlation coefficient. The respiratory rate and cardiac rate were recorded in the 0.18–0.25 Hz and 0.9–1.1 Hz ranges, re-

←

Fig 1.　Continued. The color scale for the task-activation map refers to z scores (red z, 3.5; yellow z, 5.5), and that for the resting-state map refers to correlation coefficients (red, 0.5; yellow, 0.7). The MR pulse sequence parameters are 2000/50/82 (TR/TE/flip angle) for fMR and 400/50/50 for fcMR.

Fig 2.　Consecutive coronal images showing task activation for the visual task (top) and connectivity for the visual cortex in resting-state (bottom). The task produces activation in the striate cortex region. The voxels with connectivity to the seed voxel (*crosshairs*) appear to lie in similar locations in the striate cortex region. The color scale for the task-activation map refers to z scores (red z, 3.5; yellow z, 5.5), and that for the resting-state map refers to correlation coefficients (red, 0.6; yellow, 0.8). The MR pulse sequence parameters are as in Figure 1.

Fig 3.　A selected coronal fMR map of voxels activated by the bilateral finger-tapping task (top) and of voxels functionally connected to an ROI of 2 × 2-seed voxels (*crosshairs*) in the sensorimotor cortex in a resting acquisition (bottom). The sensorimotor cortex is identified in both the fMR and the fcMR imaging. Not shown are voxels within the dentate nucleus of the cerebellum that were identified with fMR but not with the functional connectivity study. The color scale for the task-activation map refers to z scores (red z, 3.5; yellow z, 5.5), and that for the resting-state map refers to correlation coefficients (red, 0.62; yellow, 0.8). The MR pulse sequence parameters are as in Figure 1.
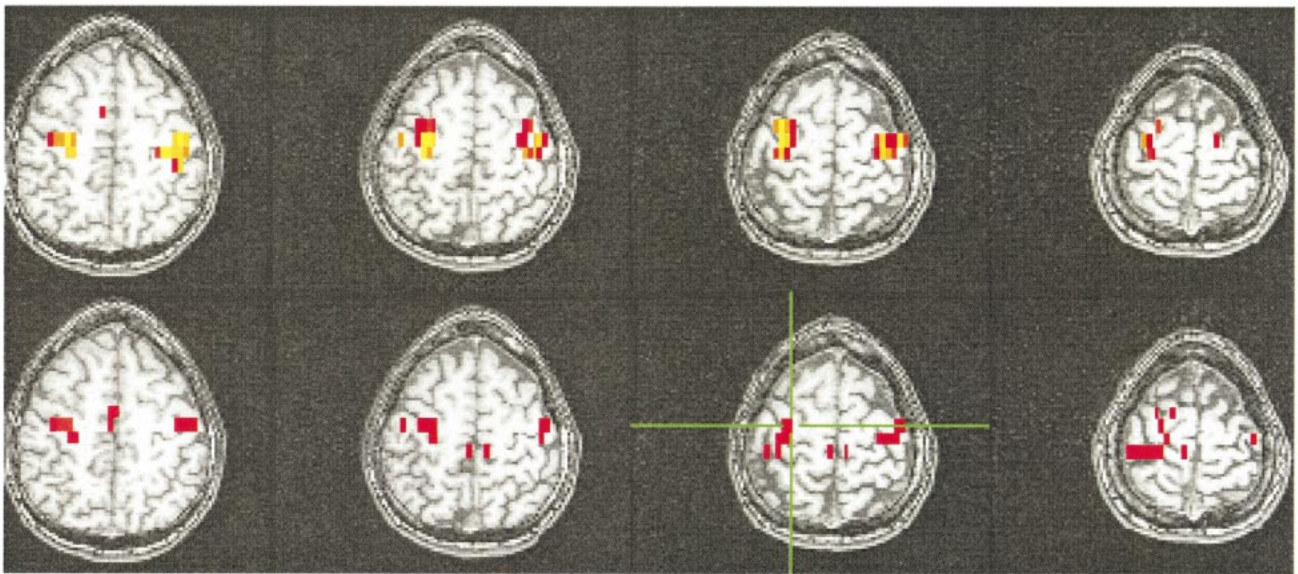
FIG 4.   A selected axial fMR map of voxels activated by the bilateral finger-tapping task (top) and of the voxels functionally connected to an ROI of 2 × 2-seed voxels (*crosshairs*) in the sensorimotor cortex in a resting-state acquisition (bottom). The sensorimotor cortex is identified in both the fMR and the fcMR maps. The SMA is not activated by the paradigm, but connectivity is clearly seen. The color scale for the task-activation map refers to z scores (red z, 3.5; yellow z, 5.5), and that for the resting-state map refers to correlation coefficients (red, 0.62; yellow, 0.8). The MR pulse sequence parameters are as in Figure 1.
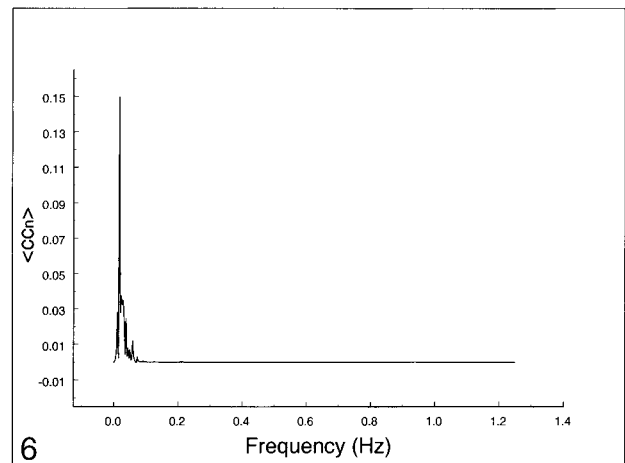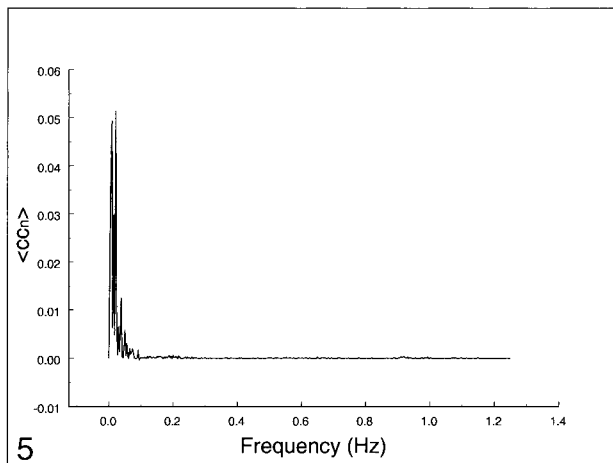

FIG 5.   Spectral analysis of the average correlation coefficient for interregional connectivity in the auditory cortex (same subject illustrated in Figure 1). Only frequency components between 0 and 0.05 Hz contribute significantly to the correlation coefficient.

FIG 6.   Spectral analysis of the average correlation coefficient for interregional connectivity in the striate cortex (same subject illustrated in Figure 2). Only frequency components less than 0.05 Hz contribute significantly to the correlation coefficient.

spectively. Contribution from respiratory and cardiac noise sources was virtually absent. Motor cortex functional connectivity (Fig 7) also had dominant contributions from low-frequency fluctuations. Small effects of respiratory contributions were visible at 0.2 Hz (fundamental frequency) and 0.4 Hz (first harmonic). The cardiac contribution at 0.93 Hz was extremely small.

The frequency spectrum of seed voxels in the left internal carotid artery showed dominant peaks at the cardiac frequency at 0.93 Hz and its first harmonic, aliased at 0.65 Hz (Figs 8–10). Low-frequency contributions and respiratory effects were small. For seed voxels in the left internal jugular

vein, mostly respiratory and low frequency bands were visible as well as some cardiac contributions. Seed voxels representing cerebrospinal fluid showed many frequency bands across the whole spectrum, mostly arising from respiratory and cardiac pulsations.

Figure 11 compares the relative contribution to the total cross-correlation coefficient of three different frequency ranges (low frequencies, 0–0.1 Hz; respiratory frequencies, 0.1–0.5 Hz; and cardiac frequencies, 0.6–1.1 Hz). Low frequencies contributed more than 90% to fcMR maps for auditory and visual connectivity and 75% for motor connectivity. For seed voxels in arteries, veins, or
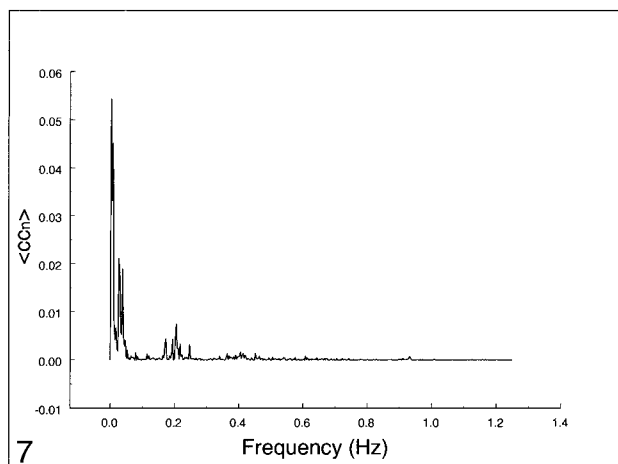
FIG 7. Spectral analysis of the average correlation coefficient for interregional connectivity in the motor cortex (same subject illustrated in Figure 3). Only the same low-frequency components contribute significantly to the correlation coefficient.
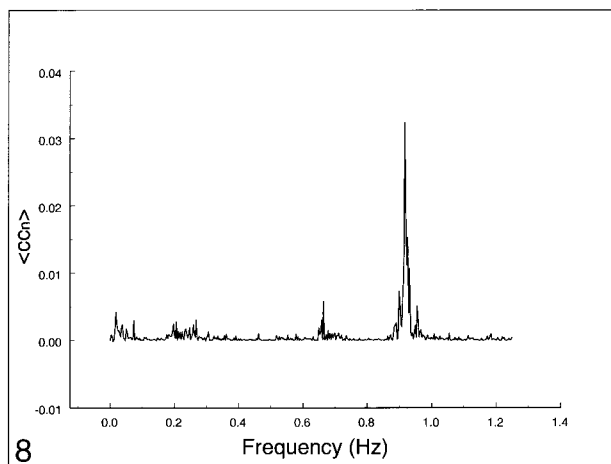
FIG 8. Spectral analysis of the average correlation coefficient obtained using a seed voxel in the right internal carotid artery. Low frequencies do not predominate. The main peak occurs at the cardiac frequency (0.93 Hz); the first harmonic is aliased to 0.65 Hz. A respiratory band is seen at 0.2 Hz.
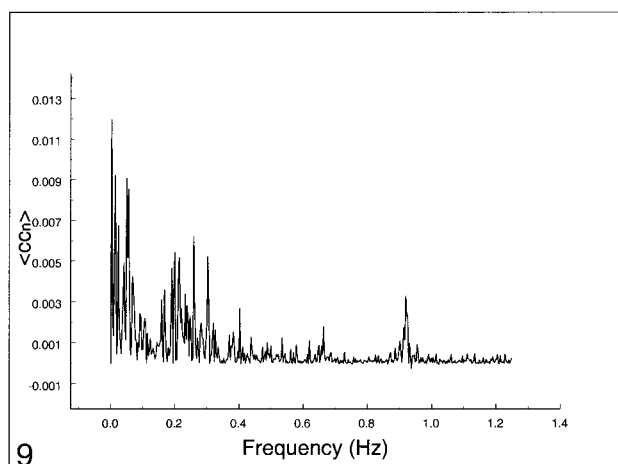

FIG 9. Spectral analysis of the average correlation coefficient from a seed voxel in the left jugular vein. Note the spread over many frequencies up to 0.4 Hz and the cardiac peaks at 0.93 Hz and 0.65 Hz.
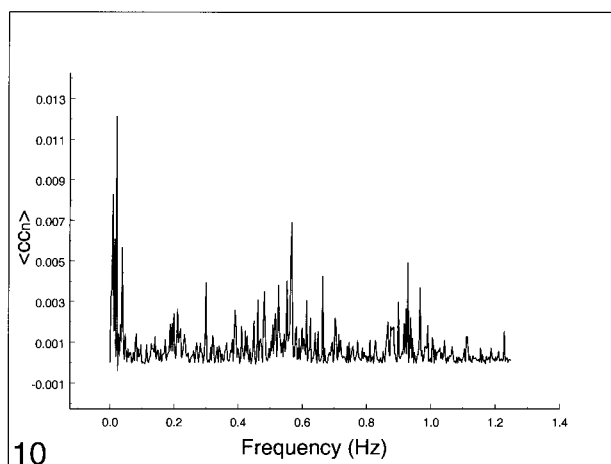
FIG 10. Spectral analysis of the average correlation coefficient obtained using a seed voxel in the left ventricle. Note the spread over many frequencies. The cardiac bands show a large spread compared with other tissue. Low-frequency peaks are visible at 0.03 Hz.
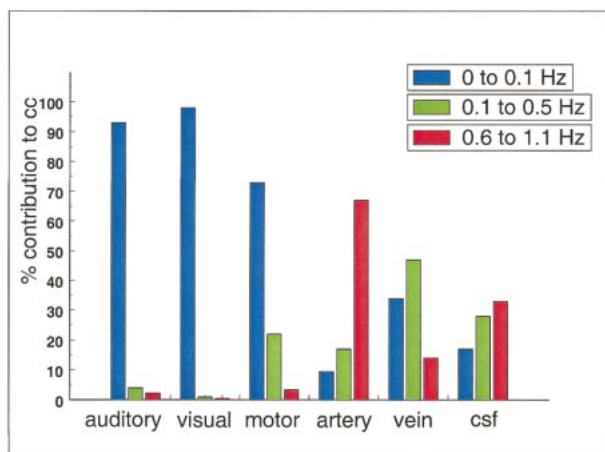
FIG 11. Contribution of low frequencies (0 to 0.1 Hz), respiratory frequencies (0.1 to 0.5 Hz), and cardiac frequencies to the cross-correlation coefficient in different ROIs in the same subject. Low-frequency components clearly dominate, contributing to functional connectivity in auditory, visual, and motor cortices. For blood vessels and cerebrospinal fluid, low-frequency components are present, but cardiac and respiratory noise sources are the main contributors.

cerebrospinal fluid, the dominant contributions were either from cardiac pulsations (70% for artery, 35% for cerebrospinal fluid) or from respiratory effects (50% for veins) but less from low-frequency fluctuations.

Discussion

The present study shows that the major frequency contributions to resting-state functional connectivity come from fluctuations less than 0.1 Hz. These fluctuations occur synchronously in functionally connected regions. Physiological noise sources, such as respiratory or cardiac pulsations, contribute little to the cross-correlation coefficient. Functionally connected regions can be identified by resting-state fcMR imaging of auditory, visual, and sensorimotor cortices.

Our method of analysis characterizes the frequencies that contribute to resting-state multislice correlation maps. Combining a sufficiently high sampling rate (TR, 400 ms) that still allows multislice imaging with a method to separate the cross-correlation maps into frequency components, we can resolve the fundamental and first-harmonic frequencies of respiratory and cardiac noise sources. The fundamental frequency and first harmonic of the respiratory cycle occur at about 0.25 and 0.5 Hz, respectively. The cardiac rate appears around 0.9 Hz, whereas the first harmonic is aliased to 0.65 Hz. We observed only minor variations depending on the subject. The recorded pulse oximeter rates varied by ±3 beats per minute and agreed well with the extent of the frequency bands in the MR data. Therefore, none of the physiological noise sources aliased into the low-frequency range (≤0.1 Hz) thought to be responsible for functional connectivity. All physiological noise sources can be identified easily.

For visual, somatosensory and auditory cortex, the separation of the fcMR maps into frequency components reveals that low-frequency fluctuations contribute much more to the correlation coefficient than do any respiratory or cardiac noise sources. For example, in functional connectivity of the auditory and visual cortices, low-frequency fluctuations contribute more than 90%; in the motor cortex, they contribute more than 85% in a typical subject. Other subjects show similar and sometimes even higher contributions of low-frequency fluctuations. Contaminations of the cross-correlation coefficient from cardiac pulsations counting all frequencies between 0.6 and 1.1 Hz are less than 5% in all subjects (average, 3%). Respiratory contamination between 0.1 and 0.5 Hz is as high as 20% in a single subject. On average, across all subjects, respiratory effects are about 15%. This finding strongly suggests that low-frequency fluctuations in functionally connected brain regions have a high degree of temporal correlation. Our finding is consistent with other reports in which low-frequency fluctuations less than 0.1 Hz in functionally related

brain regions showed a high degree of temporal correlation.

The frequency spectrum from the large blood vessels or cerebrospinal fluid has very different features. Here, low-frequency contributions are small, and respiratory and cardiac components dominate. For example, seed voxels from the internal carotid artery show an average 70% contribution from cardiac frequencies to the cross-correlation coefficient, whereas seed voxels from the jugular vein show significant contribution from respiratory frequencies. Seed voxels in cerebrospinal fluid show many different frequencies in the cross-correlation spectrum, mostly from respiratory and cardiac pulsations and less from low-frequency oscillations.

Spatial maps of task-induced fMR and resting-state fcMR imaging show many similarities. Functional cortices can be identified with both methods. However, fcMR is not intended to be a replacement for task-activated fMR. Temporal correlations in the resting state imply phase-locked neuronal activity in functionally related regions. Task-induced activation maps involve coordinated activity of several brain systems and might not reflect direct neuronal interconnections.

One limitation of our study is the potential bias in the selection of the seed voxels. The fcMR maps vary to some degree with the voxels chosen as seed voxels. For example, the respiratory band is seen clearly in Figure 7 (motor cortex) but less so in Figures 5 and 6, because of partial-volume effects. At a voxel size of $3.75 \times 3.75 \times 7$ mm^3, cerebrospinal fluid and large blood vessels might contribute to the MR signal depending on the location of the seed voxels. The contributions of large blood vessels and cerebrospinal fluid vary between voxels; thus the frequencies represented in individual voxels may vary. We reduced these biasing effects by calculating the autocorrelation function of each seed voxel time course and choosing seed voxels with similar degrees of freedom near a region showing maximum task activation in fMR imaging. The freedom to choose seed voxels on the basis of anatomic landmarks increased the chance of identifying regions with functional connectivity. Further studies are required to clarify the consistency and applicability of resting-state fcMR imaging. For future research, our method might be an important tool to probe the strength of cortical neuronal connections in healthy subjects and patients who suffer from disconnection syndromes (15–18).

Our data were derived using a high sampling rate to eliminate problems with aliasing of physiological noise sources. The limitation, compared with studies using low sampling rates, is that only four slices can be collected at a TR of 400 ms. The implication is that functional connectivity throughout the whole brain cannot be obtained with our sampling rate. Also, some aliasing of higher-order harmonics of the cardiac frequency still will occur, but the amplitudes of higher harmonics tend to decrease quickly with the order of the harmonic, and

the contribution to the cross-correlation coefficient is expected to be negligible.

An interesting point of discussion is the possibility that non-task-induced functional connectivity might contribute to task-induced activation in a functional image. The fundamental frequency of the usual task paradigm (0.016 Hz) falls directly into the low-frequency band (<0.1 Hz) responsible for functional connectivity. We found in one subject that the fundamental frequency of task-induced activation in the primary auditory cortex had an amplitude 6.8 times greater than the resting-state low-frequency oscillation in the same region. Assuming perfect phase synchrony between the oscillations from functional connectivity and task-induced signal changes, we can hypothesize that functional connectivity might contribute about 15% to an activation map. However, it is unclear how much the amplitude of the low-frequency oscillations responsible for functional connectivity might change during the performance of a task and what the phase relationship is compared with the task-induced frequency. Further studies are needed to clarify this point.

Conclusion

The methods described herein quantify the contribution of low-frequency fluctuations and physiological noise to cross-correlation functional connectivity maps. Functional connectivity maps of auditory, sensory-motor, and visual cortices derived from resting-state data depend predominantly on low-frequency fluctuations and little on respiratory and cardiac noise sources when measured at a low TR. The functional organization of the cortex as revealed by fcMR closely resembles that shown by task-activation maps. Our observations indicate that low-frequency fluctuations are a general phenomenon in eloquent cortex. Therefore, fcMR imaging may be a useful method to evaluate the strength of neuronal connections in healthy individuals and in patients with neurologic disorders.

References

1. Haughton VM, Biswal B. **Clinical application of basal regional cerebral blood flow fluctuation measurements by FMRI.** In: Hudetz A, Bruley D, eds. *Oxygen Transport to Tissue.* New York: Plenum Publishing Corp.; 1998:583–590
2. Biswal B, Yetkin FZ, Haughton VM, Hyde JS. **Functional connectivity in the motor cortex of resting human brain using echo-planar MR imaging.** *Magn Reson Med* 1995;34:537–541
3. Lowe MJ, Mock BJ, Sorenson JA. **Functional connectivity in single and multislice echoplanar imaging using resting state fluctuations.** *Neuroimage* 1998;7:119–132
4. Lowe MJ, Mock BJ, Sorenson JA. **Resting state fMRI signal correlation in multi-slice.** *Neuroimage* 1996;3:S257
5. Xiong J, Parsons LM, Gao JH, Fox PT. **Interregional connectivity to primary motor cortex revealed using MRI resting state images.** *Hum Brain Mapp* 1999;8:151–156
6. Cordes D, Haughton VM, Arfanakis K, et al. **Mapping functionally related regions of brain with functional connectivity MRI (fcMRI).** *AJNR Am J Neuroradiol* 2000;21:1636–1644
7. Arfanakis K, Cordes D, Haughton VM, Meyerand ME. **Functional connectivity after removal of task-related activation using independent component analysis.** *Proc ISMRM* 2000;241
8. Meyerand ME, Moritz CH, Arfanakis K, Cordes D, Haughton VM. **A power spectrum analysis of the low frequency resting-state fMRI signal.** *Proceedings of the World Congress Meeting 2000,* Chicago.
9. Lowe MJ, Sorenson JA. **Spatially filtering functional magnetic resonance imaging data.** *Magn Reson Med* 1997;37:723–729
10. Russel DP. **A generalized approach to time-course analysis of functional MRI of the human brain.** *Proceedings of the SMR 2nd Annual Meeting,* San Francisco, 1994:636
11. Lowe MJ, Russel DP. **Treatment of baseline drifts in fMRI time series analysis.** *J Comput Assist Tomogr* 1999;23:463–473
12. Sprent P. *Applied Nonparametric Statistical Methods.* London: Chapman and Hall;1993
13. Holmes AP, Blair RC, Watson DG, Ford I. **Nonparametric analysis of statistic images from functional mapping experiments.** *J Cereb Blood Flow Metab* 1996;16:7–22
14. Friston KJ, Holmes AP, Poline JB, et al. **Analysis of fMRI time-series revisited.** *Neuroimage* 1995;2:45–53
15. Meyerand ME, Moritz CH, Cordes D, Quigley M, Haughton VM. **Functional connectivity in the cortical and subcortical regions of the motor system.** *Proc ISMRM 8th Annual Meeting,* Denver, 2000:609
16. Lowe MJ, Phillips MD, Mattson DH, et al. **Resting state BOLD fluctuations reflect impaired functional connectivity in multiple sclerosis.** *Proc ISMRM 8th Annual Meeting,* Denver, 2000:872
17. Biswal B, Hudetz AG, Yetkin FZ, Haughton VM, Hyde JS. **Hypercapnia reversibly suppresses low-frequency fluctuations in the human motor cortex during rest using echo-planar MRI.** *J Cereb Blood Flow Metab* 1997;17:301–308
18. Geschwind N. **Disconnection syndromes in animals and man.** *Brain* 1965;88:231–294